Miscibility in Crystalline Polymer Blends: Isotactic Polypropylene and Linear Low-Density Polyethylene

Giuliana Gorrasi,[1] Rachele Pucciariello,[2] Vincenzo Villani,[2] Vittoria Vittoria,[1] Sandra Belviso[2]

[1]*Dipartimento di Ingegneria Chimica ed Alimentare, Università di Salerno, Via Ponte Don Melillo, 84084 Fisciano (Salerno), Italy*
[2]*Dipartimento di Chimica, Università della Basilicata, Via N. Sauro 85, 85100 Potenza, Italy*

Received 28 January 2003; accepted 14 May 2003

ABSTRACT: The phase behavior and the crystallization kinetics of blends composed of isotactic polypropylene (iPP) and linear low-density polyethylene (LLDPE) were investigated by differential scanning calorimetry. The phase behavior indicates the formation of separate crystals of iPP and LLDPE at each investigated blend composition. The crystallization trace reveals that iPP crystallizes in its normal range of temperatures (i.e., at temperatures higher than that of LLDPE), when its content in the blend is higher than 25% by weight. In the blend whose iPP content is as high as 25%, at least a portion of iPP crystallizes at temperatures lower than that of LLDPE. This behavior has been proposed by Bassett to be attributed to a change in the kind of nucleation from heterogeneous to homogeneous. From the Avrami analysis of the isothermal crystallization of iPP in the presence of molten LLDPE, n values close to 2 are always obtained. According to our previously proposed interpretation of the Avrami coefficient, it can be related to the crystallite fractal dimension, through $d = n + 1$, which gives values close to 3, according to the spherulitic observed morphology. The kinetics parameter, i.e., the half-time of crystallization, and the kinetic constant k show that a decrease in the overall rate of crystallization of iPP occurs on blending. Optical microscopy photographs, taken during the cooling of the samples from the melt, confirm the above results and show increasingly less resolved spherulite texture on increasing LLDPE content in the blend. The diffusion parameters evaluated for the neat polymers and for the blends in dichloromethane, which give information on the miscibility in the amorphous state, show that the diffusional behavior of the blends is governed by iPP, suggesting a two-phase amorphous state.
 J Appl Polym Sci 90: 3338–3346, 2003

Key words: blends; diffusion; crystallization; miscibility; fractal dimension

INTRODUCTION

Polymer blends are a subject of great interest in both scientific and industrial literature. From a technological point of view the production of blends is characterized by rapid and continuous growth. Such a development is attributed to the lower costs, fewer risks, and higher speed involved in the production of a blend with respect to the synthesis of new polymers or copolymers. Binary polymer blends can give monophasic or biphasic systems, with a total or partial segregation of the components into the phases.

The largest part of the studied systems concerns amorphous blends.[1,2] The study of blends in which a component can crystallize is complex because the amorphous component influences the crystallization thermodynamics and kinetics of the other.[3–5]

Correspondence to: R. Pucciariello (pucciariello@unibas.it).
Contract grant sponsor: Ministero dell'Università e della Ricerca Scientifica e Tecnologica (MURST); contract grant number: Cofin 99.

Blends in which both components can crystallize are even more complex because the phase separation and crystallization processes can occur simultaneously and/or in competition.

In any case, such blends are particularly interesting either for the commercial importance of crystalline polymers or for the possibility that they offer of studying the miscibility with relation to crystallinity.

Few papers have been published, most of which are very recent, on crystalline polymer blends.[6–17] Among them, polyethylene and polypropylene blends are the focus of increasing attention because such polymers are the thermoplastics of highest consumption, given their special and varied physical and mechanical properties. Furthermore, polyolefin blends attract additional interest because of the possibility of recycling the plastic wastes, thus avoiding the expensive and difficult process of component separation.

A number of studies[18–26] are available on the thermal and mechanical properties of isotactic polypropylene (iPP) blended with polyethylene (PE), although there is still a strong debate. In fact, most authors, through different techniques [mainly hot-stage optical microscopy (HSOM), dilatometry, and DSC] con-

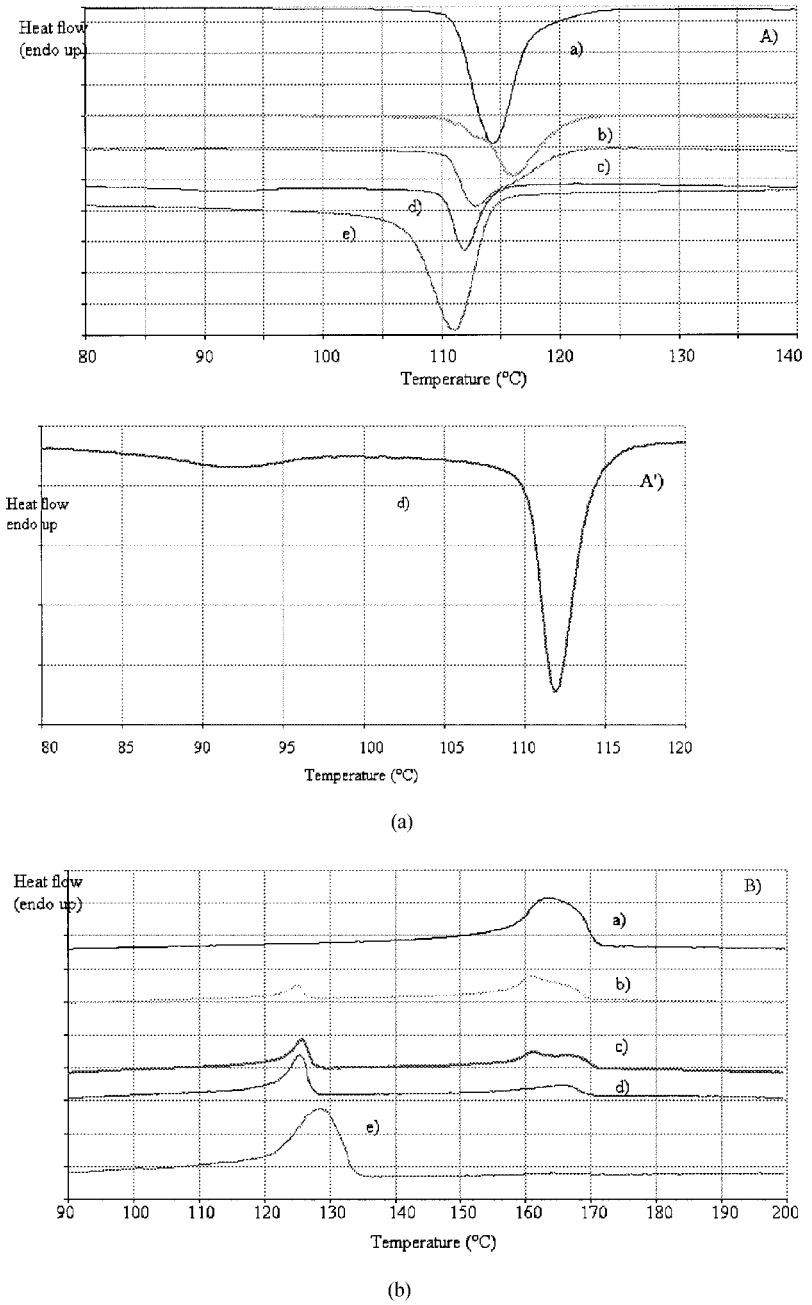

Figure 1 (A) Calorimetric curves recorded at 10°C/min on cooling from the melt iPP (a); iPP–LLDPE blends with w_{iPP} values of 0.75 (b), 0.50 (c), and 0.25 (d); and LLDPE (e). (A′) Magnification of curve (d). (B) Calorimetric curves recorded on reheating at 10°C/min melt-crystallized iPP (a); iPP–LLDPE blends with w_{iPP} values of 0.75 (b), 0.50 (c), and 0.25 (d); and LLDPE (e).

cluded that iPP crystallization is not influenced by the presence of PE,[18–24] which is an evidence of immiscibility of the two polymers not only in the crystal state but also in the melt. However, all authors agree that the addition of PE causes a reduction in the number of iPP crystallization nuclei. Other authors[25,27] claim that PE is able to delay nucleation and subsequent crystallization in PP, as a consequence of crystallization from a miscible melt, although such a miscibility would take place just in a restricted temperature range.

In this work, we studied the phase behavior of iPP–linear low-density polyethylene (LLDPE) blends at different compositions by DSC and HSOM, with the aim of gaining deeper understanding of the miscibility of the two polymers. Moreover, the crystallization kinetics of iPP in the presence of molten LLDPE was investigated. Our aim was to obtain information about the influence of LLDPE either on the rate of crystallization of iPP or on the final morphology, which are of paramount importance in defining the process and use

conditions, respectively, of materials. Up to now an in-depth study of this system has not been published.

Moreover, because the amorphous phase of polymers is the closest situation to the melt, we investigated the structural organization of the amorphous phase(s) of the blends through analysis of the diffusion parameters. A small interacting molecule, such as dichloromethane, already used as a model molecule in many structural studies, was used.[28,29]

EXPERIMENTAL

Materials

The materials used were an LLDPE (M_n 67,551; M_w 335,185) produced by Montell (Ferrara, Italy) and iPP (M_n 36,000; M_w 268,000) supplied by Statoil (Statchele, Norway). Blends of iPP–LLDPE were prepared in the molten state at high temperature (200°C), using a Brabender (Germany) CO Decoder blender, equipped with rotating blades.

The composition of the blend is reported as weight fraction (w_{iPP}) of iPP.

Thermal analysis

Thermal analysis was performed by the Perkin–Elmer DSC 7 (Perkin Elmer Cetus Instruments, Norwalk, CT). Runs were performed on 5 ± 0.5 mg samples in a nitrogen atmosphere. The apparatus was calibrated using the melting temperature of indium (156.6°C) and its heat of fusion. Before each run the baseline was optimized in the suitable temperature range and then subtracted from the corresponding DSC curve. Transition temperatures were taken as the appropriate peak temperatures in the DSC curve and are reproducible to ±0.3°C. All the experiments were performed after heating the samples to 200°C at 10°C/min and holding them at this temperature for 10 min to cancel any thermal history. The crystallization curves were obtained by cooling the sample from the melt to room temperature at 10°C/min and the melting curves on reheating it to 200°C at the same scanning rate. For the isothermal crystallizations the samples were cooled from the melt to the selected crystallization temperature T_c and taken at the same temperature for the time necessary to the completion of the crystallization of iPP. To avoid crystallization on cooling, liquid nitrogen was used as a coolant, which allows the sample to reach the selected crystallization temperature at 200°C/min. The crystallization temperatures were chosen in a suitable range to ensure that LLDPE was still completely molten. The heats of transition were calculated from the peak areas using the Pyris software running under Windows NT 5.0 on a Pentium III PC and their precision was at least

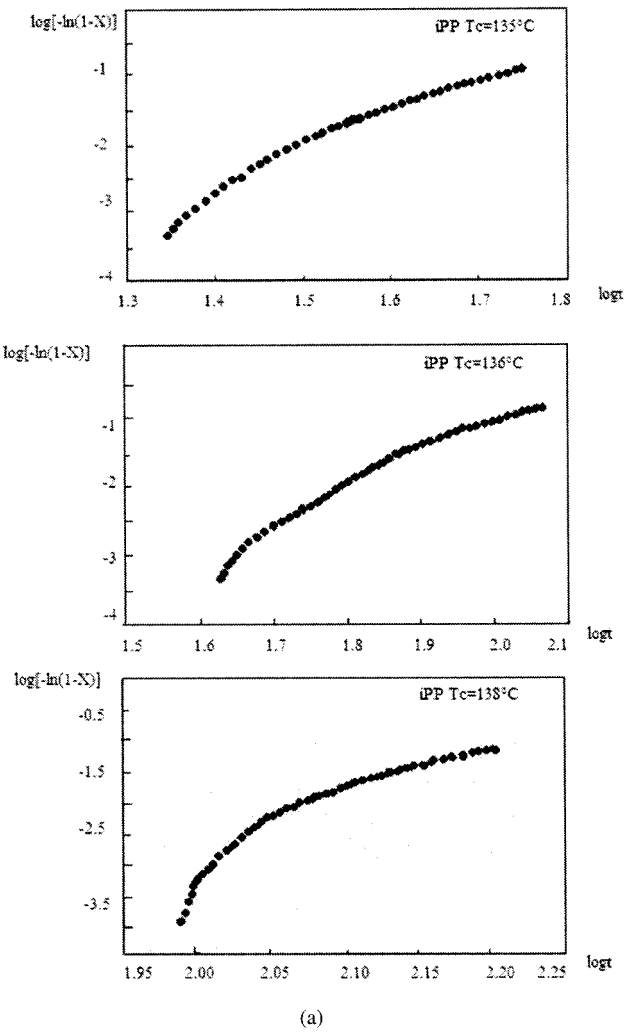

Figure 2 Trend of the crystallinity expressed as log[−ln(1 − X)] as a function of log t (where t is the crystallization time) obtained for the following isothermal crystallization from the melt at 135, 136, and 138°C: iPP and blends with w_{iPP} values of 0.75 and 0.50.

±0.1%. The heats of crystallization at suitable interval times were calculated by the method of partial areas. The heats of crystallization were converted to degrees of crystallinity using the enthalpy of fusion of a perfect crystal of iPP (209 J/g).[30]

Hot-stage polarized optical microscopy

The optical observations of the crystallization of iPP, LLDPE, and their blends as a function of the temperature were performed with an Axioplan–Zeiss (Oberkochen, Germany) polarizing microscope equipped with a Linkam microfurnace. Images were captured using a Zeiss MC80 microscope camera. Samples were examined between 16-mm-diameter silica glass plates.

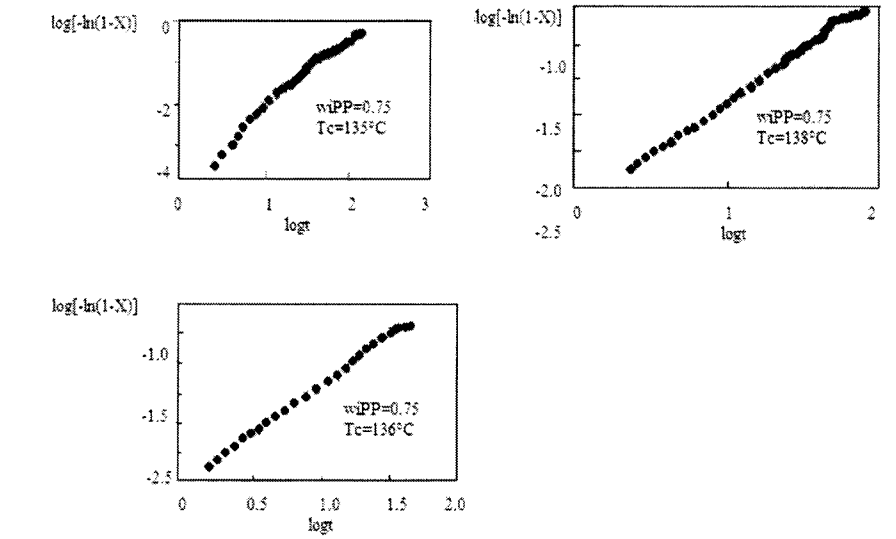

(b)

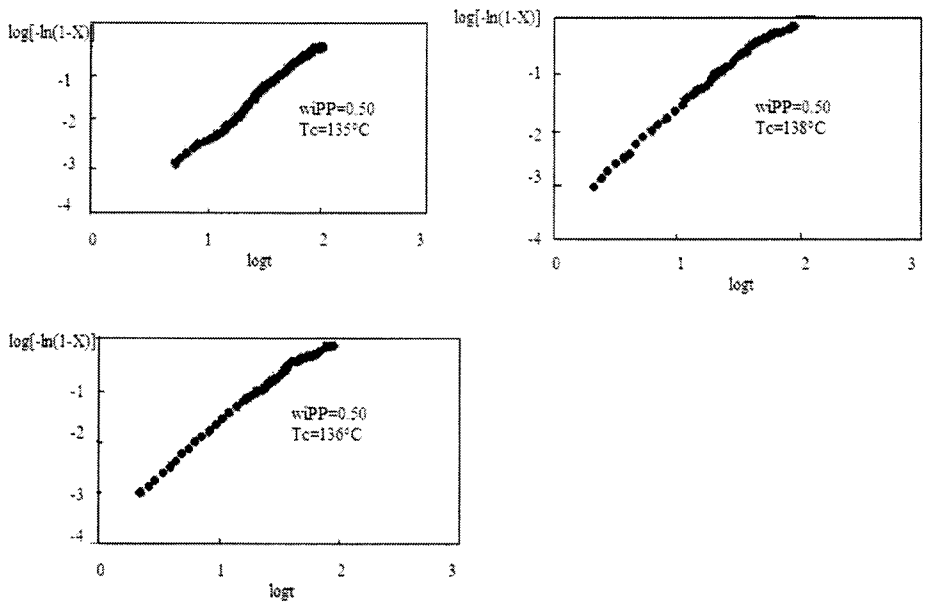

(c)

Figure 2 (*Continued from previous page*)

A thermal treatment similar to that used in calorimetric measurements was used to perform a meaningful comparison. Samples were heated at 10°C/min to 200°C and kept 10 min at that temperature before being cooled to room temperature at the same rate. The temperature on the hot stage can be kept constant to within ±0.1°C.

Transport properties of the film obtained from the blends

Films from the blends and the pure polymers were obtained by melting the materials in a Carver Laboratory press between two Teflon sheets and slowly cooling them in air. The film thickness was about 0.1 mm. The diffusion coefficients were evaluated using the microgravimetric method, according to a previously reported procedure.[31] The samples were put into a microgravimetric balance at different vapor activities of dichloromethane ($a = P/P_0$, where P is the actual pressure to which the sample was exposed and P_0 is the saturation pressure at the test temperature) at the temperature of 25°C. The gain in weight was followed, as function of time, up to the equilibrium.

RESULTS AND DISCUSSION

Thermal behavior

In Figure 1 the calorimetric curves corresponding to crystallization and melting of the blends are reported.

For the sake of comparison the DSC curves of the neat components are also shown.

For the blends with w_{iPP} values of 0.75 and 0.50 we obtained a main peak of crystallization at about 116 and 113°C, and a shoulder at 113 and 116°C, respectively (whereas the peaks of unblended components are located at about 111°C for LLDPE and 114°C for iPP) [Fig. 1(A)]. These are the normal ranges of crystallization and melting for iPP and LLDPE; therefore the observed peaks can be attributed to the separate crystallization of the two components.

Correspondingly, two melting peaks were obtained located at about 125 and 161°C (128 and 165°C for the neat components), which are likely to correspond to separate melting of iPP and LLDPE [Fig. 1(B)]. Therefore it is apparent that in the considered blends iPP and LLDPE give complete phase separation in the crystal state.

For the blend with $w_{iPP} = 0.25$ the two polymers are still immiscible in the crystal state as confirmed by the presence of two crystallization [Fig. 1(A′)] and two melting peaks [Fig. 1(B)], whose partial areas are roughly comparable with the extent of each component in the blend (about 20 and 80%, respectively). Nevertheless the location of the two crystallization peaks is quite different from that in the previous cases. In fact the two exotherms are located near 112 and 92°C. This behavior is similar to that described by Bassett et al.[32] for a blend of iPP and branched PE at 20/80 composition. The higher temperature peak was attributed to PE and the lower peak to PP. This behavior was interpreted as crystallization from dispersions of droplets, which from morphological observations have been identified as constituted of iPP. In these systems generally heterogeneous nucleation occurs, where the nuclei are inside the droplets. Nevertheless, when the PP concentration decreases, in particular when it is about 20%, the droplets do not contain any more nuclei and a quasi-homogeneous nucleation is followed, determining solidification to occur at lower temperatures.

Similarly, we can attribute the peak at 108°C to the crystallization of LLDPE, which occurs in the normal range of temperatures, and that at 90°C to the crystallization of iPP. This result clearly indicates that the crystallization kinetics of iPP in the presence of molten LLDPE cannot be performed for this last blend, given that at least a major portion of iPP crystallizes after LLDPE. Therefore the influence of molten LLDPE on the crystallization kinetics of iPP was investigated for the blends with w_{iPP} values of 0.75 and 0.50, where iPP crystallizes at a higher temperature than does LLDPE. The isothermal crystallizations were carried out at 135, 136, and 138°C, temperatures at which the complete melting of LLDPE is ensured. The heats of crystallization evaluated at selected crystallization times were converted to degrees of crystallinity X using the enthalpy of fusion of a perfect iPP crystal. It is well known that the overall isothermal crystallization rate, as the development of crystallinity versus time, can be described by the Avrami equation,[33] which in its logarithmic form reads as

$$\log[-\ln(1 - X)] = n \log t + \log k$$

where X is the degree of crystallinity developed at time t, k contains the rate constants of nucleation and crystal growth, and n reflects the type of nucleation and the habit of the growing nuclei.

In Figure 2 we report the calorimetric data as $\log[-\ln(1 - X)]$ versus $\log t$ for unblended iPP and for the blends with w_{iPP} values of 0.75 and 0.50. For neat iPP (Fig. 2) the Avrami plots appear as usual: a first linear trend up to about 30% crystallinity, followed by a decrease in the slope. For the blends (Fig. 2) the same trend is obtained for the lower crystallization temperatures, whereas at the higher temperature no change in the slope takes place.

In Table I we report the Avrami exponent n evaluated, as usual, through the linear fitting of the first portion of the curve (i.e., up to 30% crystallinity) $\log[-\ln(1 - X)]$ versus time in the case where a change in slope occurs, and of the whole curve in the case where the change does not occur. The values of n vary slightly, but in general are very close to 2. They are in very good agreement with those found by Li et al.[27] by optical microscopy for blends containing 20 wt % of iPP. A value of 2 for the Avrami exponent has been suggested to be related to heterogeneous nucleation and bidimensional growth.[34] Nevertheless, as shown in the following, and as reported in the literature for similar blends, a spherulitic morphology was observed.[25,27,32] In a previous study[35] we proposed that the Avrami exponent can be correlated to the fractal dimension of the crystallites d according to $d = n + 1$. In our case we obtained $d \cong 3$, which is in agreement with the observed spherulitic morphology.

The practically coincident values of n for neat iPP and for blended iPP suggest that a similar morphology, with respect to the shape of the crystallites is concerned, takes place in the crystalline state of the investigated systems. Therefore, the presence of molten LLDPE seems to scarcely influence the shape of iPP crystallites.

In Figure 3 we reported $\log k$, as obtained from the fitting of the first linear part of the Avrami plots, as a function of $1/T_c$ and in Figure 4 the crystallization half-time $t_{1/2}$, that is, the time needed for the crystallinity to reach half of the final value at the selected crystallization temperature. They increase, as expected, as T_c increases, and are higher for the blends

TABLE I
Kinetic Parameters, Evaluated from the Avrami Analysis, for Neat iPP and for Blends with w_{iPP} Values of 0.75 and 0.50

W_{iPP}	T_c (°C)	$t_{1/2}$ (min)	$-\log k$	n
1.0	135	66	3.1	1.8
	136	67	3.1	1.8
	138	86	3.4	1.8
	140	244	4.1	1.9
0.75	135	64	3.0	1.9
	136	103	3.5	2.0
	138	154	3.6	2.0
0.50	135	60	2.7	1.7
	136	89	3.9	2.0
	138	138	4.2	1.9

than for neat iPP, especially in the case of $t_{1/2}$. These trends show that a decrease in the crystallization of iPP occurs upon blending. As previously reported, all authors agree that in other iPP–LLDPE blends a decrease in the crystallization of iPP in the presence of molten PE is attributable only to a reduction in the nuclei density, which takes place from immiscible melts. Li et al.[27] suggested that iPP and LLDPE are miscible in the molten state, when the content of iPP in the blend is 20% by weight. In our case the situation appears more complex; in fact, as previously discussed, for $w_{iPP} = 0.25$, at least a portion of iPP crystallizes at temperatures lower than the LLDPE. This behavior was interpreted by Bassett for similar systems[32] as crystallization in small droplets, which is typical of crystallization from immiscible melts.

On the basis of such results iPP and LLDPE seem to be immiscible in the molten state, the delay in the crystallization rate of iPP in the presence of molten LLDPE mainly being the result of a decrease in the nuclei density.

Hot-stage polarized optical microscopy

In Figure 5(A)–(C) optical microscopy photographs taken at different times during the crystallization of neat iPP during the cooling from the melt at 10°C/min are reported. The spherulites of iPP appear as bright circular areas under polarized light in the dark background and show the distinctive Maltese cross.

For blends with w_{iPP} values of 0.75 and 0.50 similar spherulite structures are observed [Fig. 5(D), (E)]. Nevertheless, the spherulites appear less resolved than those in neat iPP, although they can still be distinguished. Moreover, if one takes into account the

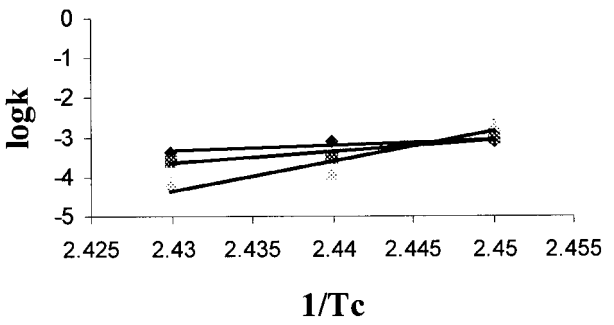

Figure 3 log k as obtained from the linear fitting of the Avrami plots as a function of $1/T_c$ for iPP (light gray symbols), and blends with w_{iPP} values of 0.75 (dark gray symbols) and 0.50 (black symbols).

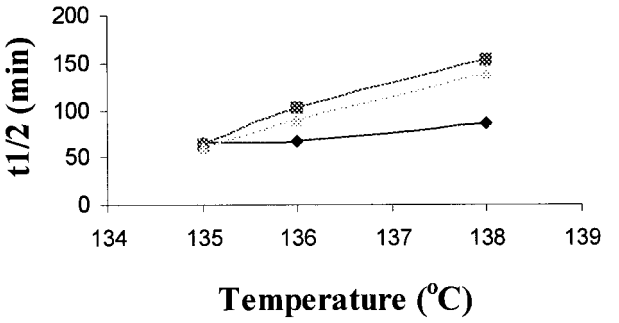

Figure 4 Half-time of crystallization $t_{1/2}$ as a function of $1/T_c$ for iPP (light gray symbols), and blends with w_{iPP} values of 0.75 (dark gray symbols) and 0.50 (black symbols).

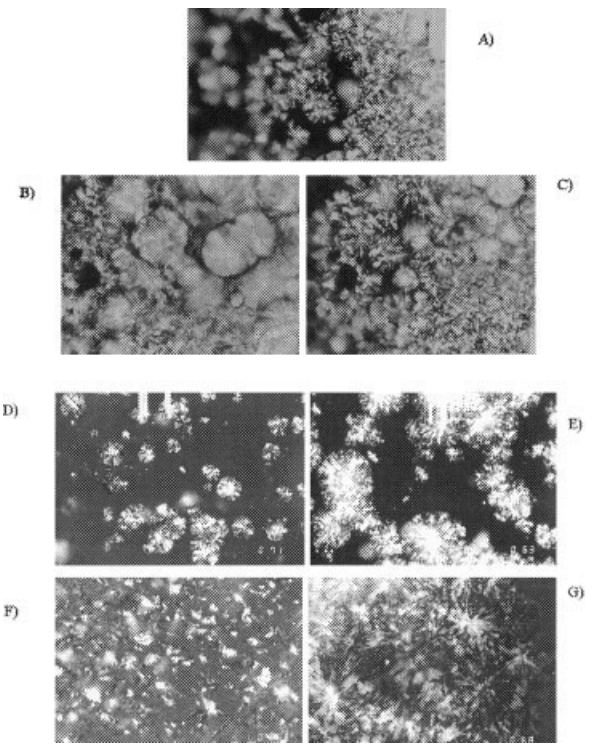

Figure 5 Hot-stage polarized microscope photographs for samples crystallized from the melt at 10°C/min for iPP at 134°C (A), 132.3°C (B), and 128.9°C (C); the blend with $w_{iPP} = 0.75$ at 118.2°C (D), with $w_{iPP} = 0.50$ at 124.5°C (E), with $w_{iPP} = 0.25$ at 122.3°C (F); and the open-arm spherulites in the case of the blend with $w_{iPP} = 0.75$ at 157.5°C (G). Magnification ×32.

temperatures at which the photographs were taken and makes a comparison with those of neat iPP, the delay in the crystallization kinetics induced by molten LLDPE, shown by the calorimetric study, can be easily confirmed. On the whole, the gross structure of LLDPE/iPP blends with w_{iPP} values of 0.75 and 0.50 is typical of iPP dispersed within an LLDPE matrix. During the cooling experiments from the melt, for concentrations of iPP above 25% in weight, heterogeneous nuclei cause iPP to crystallize in its normal range of crystallization temperatures.

For the blend with the lowest concentration of polypropylene ($w_{iPP} = 0.25$) DSC scans reveal that at least a portion of iPP crystallizes at temperatures lower than that of LLDPE. This can be attributed to the fact that the nuclei become too dispersed to cause all iPP to crystallize, so that—for the most part—it crystallizes according to a homogeneous regime, crystallizing at a lower temperature than that of polyethylene.[32] However, the optical microscopy photographs [Fig. 5(F)] reveal, also for this blend, a coarse spherulitic optical texture that begins to appear at higher temperatures than the beginning of polyethylene crystallization (i.e., in the usual polypropylene crystallization range). Nevertheless, by DSC no transition is observed at such temperatures, likely because of a low contribution to the whole crystallization heat and to the closeness of the crystallization temperatures of our samples of iPP and LLDPE.

We verified that the observed coarse spherulites are not the result of polyethylene crystallization; in fact, optical microscopy experiments on pure LLDPE show that LLDPE crystallizes at a lower temperature with respect to that corresponding to the formation of the spherulites and that it shows a different optical texture.

Figure 5(F) indicates that the spherulite structure becomes particularly irregular, small, and coarse in the blend with $w_{iPP} = 0.25$.

In all cases crystallization of iPP occurs in small droplets, which is typical for crystallization from immiscible melts. Moreover, from Figure 5(G) it can be observed that the droplets attempt to connect together to form the open-armed diffuse spherulites.

Transport properties

The diffusion parameters were evaluated at different activities of dichloromethane. At each vapor activity the sorption was reported as C_t/C_{eq}, where C_t is the concentration of vapor at time t and C_{eq} is the equilibrium value, as function of the square root of time $t^{1/2}$. The sorption curves determined at each vapor activity showed a Fickian behavior, so that it was possible to derive an average diffusion coefficient D for each vapor concentration using the following relationship[37]:

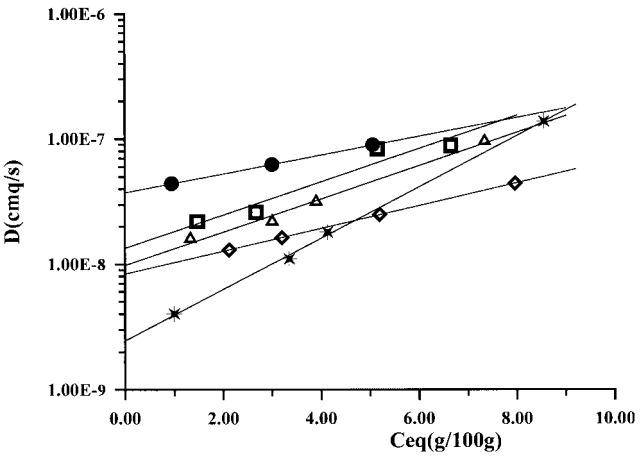

Figure 6 The diffusion coefficient D (cm^2/s) as a function of C_{eq} (g/100 g) of dichloromethane sorbed by all the film. LLDPE (●), $w_{iPP} = 0.25$ (□), $w_{iPP} = 0.50$ (△), $w_{iPP} = 0.75$ (◇), iPP (✳).

$$\frac{C_t}{C_{eq}} = \frac{4}{d}\left(\frac{\bar{D}t}{\pi}\right)^{1/2} \quad (1)$$

where d is the thickness of the sample.

Because the diffusion coefficient increases with increasing concentration, we have to determine the dependency of diffusion on concentration to extrapolate to zero penetrant concentration and obtain the thermodynamic parameter D_0, which is related to the thermodynamic state of the amorphous permeable phase. Generally the dependency of the diffusion on concentration follows the empirical law[38]

$$D = D_0 \exp(\gamma C_{eq}) \quad (2)$$

where D_0 is related to the fractional free volume and to the thermodynamic state of the permeable phase; and γ, the concentration coefficient, is correlated to the effectiveness of the penetrant in plasticizing the polymer.

Figure 6 reports D as a function of C_{eq} of vapor sorbed for the pure polymer and the three blends. The diffusion parameters are dependent on concentration, according to eq. (2), and for each sample it was possible to determine the zero diffusion coefficient D_0. D_0 as a function of iPP weight percentage is reported in Figure 7. It is interesting to note that the decrement of D_0, going from the pure LLDPE to the pure iPP, is relevant already with the presence of 25% of iPP in the blend. This result suggests that the two amorphous phases are "segregated" and combined as resistances in series with respect to the mass flow. In such a configuration, the controlling mechanism is the diffusion through the material having the largest resistance to mass flow. As from Figure 7, iPP shows the lowest

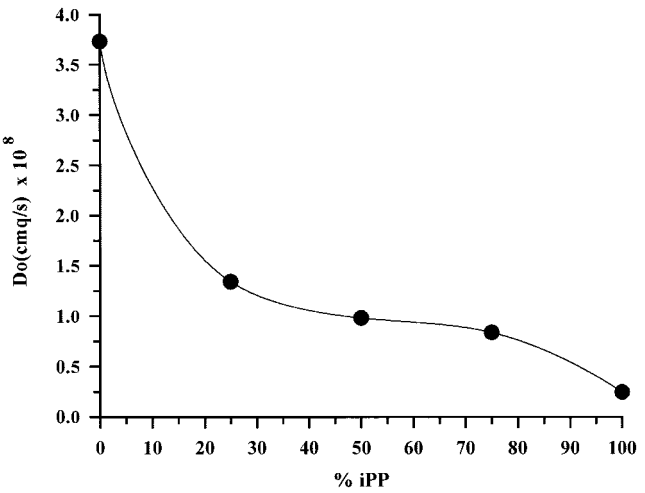

Figure 7 The zero diffusion coefficient $D_0 \times 10^8$ (cm^2/s) as a function of iPP percentage.

zero diffusion coefficient, so it determines the diffusional behavior of all the blends.

CONCLUSIONS

The study of the phase behavior in blends of iPP and LLDPE shows that the two polymers crystallize separately, independent of the blend composition. Nevertheless, the crystallization behavior of iPP is strongly affected by the presence of LLDPE. In particular, the blend composition is determined upon iPP crystallization. In fact when w_{iPP} in the blend becomes as low as 0.25, the majority of iPP does not crystallize in its normal range of temperatures (i.e., at temperatures higher than that of LLDPE), but at lower temperatures. This behavior can be ascribed to a change from heterogeneous to homogeneous nucleation inside iPP droplets, which causes a different crystal morphology.

The study of the crystallization kinetics of iPP at temperatures where LLDPE is in the molten state shows that LLDPE induces a delay in the crystallization of iPP. In fact, the Avrami constant k and especially the crystallization half-time increase on increasing the LLDPE content in the blends. In contrast, the parameter n is always the same (~ 2) and, according to our previous interpretation, can be related to the crystal fractal dimension through $d = n + 1$, which is in agreement with a nearly spherical morphology.

The constancy of n, and then of d, reveals that the presence of LLDPE does not influence the gross shape (close to spherical) of the crystallites, although optical microscopy observations show that, on increasing the content of LLDPE in the blend, the spherulites, although always present, become more irregular, smaller, and coarser.

The above results suggest immiscibility in the crystal state, as expected, but also in the melt, the delay induced by LLDPE on the crystallization rate of iPP being attributable essentially to a reduction in the nuclei density. The study of the transport properties indicates that the diffusion in the blends is governed by iPP, confirming the immiscibility in the amorphous phase.

A MURST grant ("Interfasi polimeriche e cristallizzazione," Cofin 99) is gratefully acknowledged.

References

1. Olabisi, O.; Robeson, L. M.; Shaw, M. T. Polymer–Polymer Miscibility; Academic Press: New York, 1979.
2. Paul, D. R.; Barlow, J. W. J Macromol Sci Rev Macromol Chem 1980, 18, 109.
3. Paul, D. R.; Barlow, J. W. In: Polymer Science and Technology; Lempner, D.; Grisch, K. G., Eds.; Plenum Press: New York, 1980; Vol. 11, p. 239.
4. Runt, J. P.; Martynowicz, L. M. In: Multicomponent Polymer Materials; Paul, D. R.; Sperling, L. H., Eds.; American Chemical Society: Washington, DC, 1986; Chapter 7, p. 111.
5. Starkweather, H. W. In: Polymer Compatibility and Incompatibility; Solc, K., Ed.; Harwood: New York, 1982; pp. 383–395.
6. Hu, S. R.; Kyu, T.; Stein, R. S. J. J Polym Sci Part B: Polym Phys 1987, 25, 71.
7. Alamo, R. G.; Flaser, R. H.; Mandelkern, L. J Polym Sci Part B: Polym Phys 1988, 26, 2169.
8. Martinez Salazar, J.; Sanchez Cuesta, M.; Plans, J. Polymer 1991, 32, 2984.
9. Hill, M. J.; Barham, P. J.; Keller, A. Polymer 1992, 33, 2530.
10. Tashiro, K.; Izuchi, M.; Kobayashi, M.; Stein, R. S. Macromolecules 1994, 27, 1221.
11. Natta, G.; Allegra, G.; Bassi, I. W.; Sianesi, D.; Caporiccio, G.; Torti, E. J Polym Sci Part A: Polym Chem 1965, 3, 4263.
12. Guerra, G.; Karasz, F. E.; MacKnight, W. J. Macromolecules 1986, 19, 1935.
13. Tanaka, H.; Lovinger, A. J.; Davis, D. D. J Polym Sci Part B: Polym Phys 1990, 28, 2183.
14. Runt, J.; Jin, L.; Talibuddin, S.; Davis, C. R. Macromolecules 1995, 28, 2781.
15. Hill, M. J.; Barham, P. J.; Keller, A.; Rosney, C. C. A. Polymer 1991, 32, 1384.
16. Hill, M. J.; Barham, P. J.; Keller, A.; Rosney, C. C. A. J Mater Sci Lett 1988, 7, 1271.
17. Alamo, R. G.; Londono, J. D.; Mandelkern, L.; Stehling, F. C.; Wignall, G. D. Macromolecules 1994, 27, 411.
18. Galeski, A.; Pracella, M.; Martuscelli, E. J Polym Sci Polym Phys Ed 1984, 22, 739.
19. Galeski, A.; Bartczack, Z.; Pracella, M. Polymer 1984, 25, 1323.
20. Martuscelli, E.; Pracella, M.; Volpe, G. D.; Greco, P. Makromol Chem 1984, 185, 1041.
21. Martuscelli, E. Polym Eng Sci 1984, 24, 563.
22. Bartczak, Z.; Galeski, A.; Pracella, M. Polymer 1986, 27, 537.
23. Wenig, W.; Meyer, K. Colloid Polym Sci 1980, 258, 1009.
24. Bartczak, Z.; Galeski, A.; Martuscelli, E. Polym Eng Sci 1984, 24, 1155.
25. Long, Y.; Stachurski, Z. H.; Shanks, R. A. Prog Polym Sci 1995, 20, 651.
26. Avalos, F.; Lopez-Manchado, M. A.; Arroyo, M. Polymer 1996, 37, 5681.
27. Blom, H. P.; The, J. W.; Bremner, T.; Rudin, A. Polymer 1998, 39, 4011.

28. Li, J.; Shanks, R. A.; Long, Y. Polymer 2001, 42, 1941.
29. D'Aniello, C.; Guadagno, L.; Gorrasi, G.; Vittoria, V. Polymer 2000, 41, 2515.
30. Barra, G.; D'Aniello, C.; Guadagno, L.; Vittoria, V. J Mater Sci 1999, 34, 4601.
31. Krigbaum, W. R.; Uematsu, I. J Polym Sci Part A 1965, 3, 767.
32. Vittoria, V.; de Candia, F.; Capodanno, V.; Peterlin, A. J Polym Sci Part B: Polym Phys 1986, 24, 1009.
33. Dong, L.; Bassett, D. C.; Olley, R. H. J Macromol Sci 1998, B37, 527.
34. Avrami, M. J Chem Phys 1941, 9, 177.
35. Godovskii, Y. K. Polym Sci USSR 1969, 11, 2423.
36. Pucciariello, R.; Villani, V.; Mancusi, C. J Appl Polym Sci 1999, 74, 1607.
37. Lustiger, A.; Marzinsky, C. N.; Müeller, R. R. J Polym Sci Part B: Polym Phys 1998, 36, 2047.
38. Crank, J. The Mathematics of Diffusion; Oxford University Press: Oxford, UK, 1967; Chapter IV, p. 352.
39. Fujita, H. In: Diffusion in Polymers; Crank, J.; Park, G. S., Eds.; Academic Press: New York, 1968; pp. 1–17.